



## OPEN ACCESS

## EDITED BY

Juan Jose Munoz-Perez,  
University of Cádiz, Spain

## REVIEWED BY

Haifei Yang,  
East China Normal University, China  
Longjiang Mao,  
Nanjing University of Information Science and  
Technology, China  
Jinlong Wang,  
East China Normal University, China

## \*CORRESPONDENCE

Longsheng Wang  
✉ 52wls@163.com

RECEIVED 14 January 2024

ACCEPTED 24 May 2024

PUBLISHED 24 June 2024

## CITATION

Meng L, Wang L, Wang Q, Zhao J, Zhang G,  
Zhan C, Liu X, Cui B and Zeng L (2024)  
Geochemical characteristics of the modern  
Yellow River Delta sediments and their  
response to evolution of the  
sedimentary environment.  
*Front. Mar. Sci.* 11:1370336.  
doi: 10.3389/fmars.2024.1370336

## COPYRIGHT

© 2024 Meng, Wang, Wang, Zhao, Zhang,  
Zhan, Liu, Cui and Zeng. This is an open-  
access article distributed under the terms of  
the [Creative Commons Attribution License  
\(CC BY\)](https://creativecommons.org/licenses/by/4.0/). The use, distribution or reproduction  
in other forums is permitted, provided the  
original author(s) and the copyright owner(s)  
are credited and that the original publication  
in this journal is cited, in accordance with  
accepted academic practice. No use,  
distribution or reproduction is permitted  
which does not comply with these terms.

# Geochemical characteristics of the modern Yellow River Delta sediments and their response to evolution of the sedimentary environment

Liwei Meng<sup>1</sup>, Longsheng Wang<sup>1,2,3\*</sup>, Qing Wang<sup>1</sup>, Jiawen Zhao<sup>1</sup>,  
Guiye Zhang<sup>1</sup>, Chao Zhan<sup>1</sup>, Xianbin Liu<sup>1</sup>, Buli Cui<sup>1</sup> and Lin Zeng<sup>1</sup>

<sup>1</sup>Institute of Coastal Research, Ludong University, Yantai, China, <sup>2</sup>State Key Laboratory of Loess and Quaternary Geology, Institute of Earth Environment, Chinese Academy of Sciences, Xi'an, China,

<sup>3</sup>State Key Laboratory of Lake Science and Environment, Nanjing Institute of Geography and Limnology, Chinese Academy of Sciences, Nanjing, China

**Introduction:** Sedimentary evolution and river channel changes of large river delta (e.g. Huang River, Changjiang River) in response to environmental changes have been one of the key issues in global change research.

**Methods:** This study reconstructed sedimentary environment changes in the modern Yellow River Delta (YRD), based on grain size and elemental chemical analysis of two short cores (YDC and YDG) from the southern region of the Qing 8 course delta of the modern YRD.

**Results:** The results indicated that the cores YDC and YDG sediment were dominated by silt (58.47% and 67.6%, respectively) with varied grain-size variations and poor sediment sorting. The cores YDC and YDG sediments are both predominantly composed of the major element SiO<sub>2</sub>, and have an average content of 55.53% and 58.45%, respectively. The R-mode factor analysis showed the content of chemical substances of core sediments was controlled by three factors: grain size, sedimentary provenance, and marine sedimentary dynamics.

**Discussion:** Before the diversion of the Yellow River to the Qing 8 course in 1996, the two cores sediment were mainly sources from the Yellow River, and both cores were in the delta-front sedimentary environment under weak hydrodynamic conditions. After the Yellow River was diverted to the Qing 8 course, the cores YDC and YDG experienced significant erosion under the nearshore strong waves and tides. And then the sedimentary environment of the YRD changed from siltation to erosion. The results of the study would help to further our understanding of the changes in sediment grain size and geochemical element characteristics in the Yellow River estuary, and reveal the evolution of its sedimentary environment.

## KEYWORDS

sediment grain size, geochemical elements, sedimentary environment, river channel change, Yellow River delta

## 1 Introduction

The delta region is located in the area of ocean-land interaction, which is very sensitive to global and regional climate and environmental changes (Milliman and Meade, 1983; Dethier et al., 2022). Simultaneously, climatic change and sea level fluctuation have emerged as major natural forces affecting the development of human civilization. Their patterns of development and mechanisms of influence have received considerable attention (Wang et al., 2010; Wu et al., 2020; Hou et al., 2021). The Yellow River Delta (YRD) is one of the most sensitive zone for land-sea interactions in the world, which is characterized by high frequent channel migration in the Yellow River estuary (Jiang et al., 2018; Wu et al., 2020). In addition, the silted coastline of the estuary is being pushed seawards by the mass sediment supply from the Yellow River, while oceanic dynamics (waves and tides) are simultaneously causing coastal erosion and retreat (Li et al., 1998; Xu, 2000; Wang et al., 2010). Over the decades, climate change and extensive human activities within the river basin have greatly alternated estuary sediment concentrations and the balance of river-ocean dynamics, resulting in changes of sedimentary transportation and sedimentary patterns of YRD estuary (Hou et al., 2021; Liu et al., 2022; Li et al., 2023b, Li et al., 2023b).

Geochemical elements are widely used as proxy of sedimentary environmental evolution. The geochemical characteristics of sediments are the response for the changes of the environment, which they can provide an important basis for distinguish sedimentary environments and the process of environmental evolution (Cao, 1992; Cui et al., 2017; Zhang et al., 2013; Cai et al., 2018; Ling et al., 2021; Tursun et al., 2022; Liu et al., 2023). The Yellow River is a major conduit for the transport of erosive sediments from land to sea. And the sediment delivered by Yellow River to the ocean mostly deposits in YRD. The YRD are both 'drivers' and 'recorders' of sedimentary sources and regional environmental change changes. Numerous scholars have conducted extensive research on sediment transport and sedimentation in the modern YRD and its adjacent marine environments (Zhao et al., 2016; Pang et al., 2022). Pang et al. (2022) conducted a study on the distribution characteristics of sediment geochemical elements in the Ningxia-Inner Mongolia section of the Yellow River, revealing the complex interaction between aeolian-sand and flow-sand processes. The spatial distribution of chemical elements demonstrated noticeable variations over distance, which was contributed to climatic changes, source-rock composition, and sediment provenance variation. Zhao et al. (2016) employed the Q-mode method to investigate the geochemical zoning of surface sediments of the modern YRD. The results showed that the concentrations and spatial patterns of chemical elements were significantly influenced by grain size. Over the past decades, geochemical element proxy (e.g. trace element B, B/Ga and Sr/Ba ratios) have been extensively utilized in variations sedimentary environment (e.g. lakes, loess and peat) to paleoclimate reconstructions. In addition, previous studies indicates that the content and distribution of geochemical elements can also significantly influenced by sediment grain size (Zhao et al., 2016). The relationship between grain size and elemental composition in estuarine sediments is complex and varies among different elements. Normally, finer-grain sediments tends to have higher concentrations

of Fe, Mn, Cu, and Zn, especially in clay-sized particles, while coarse grain sediment tends to have higher concentrations of Si. However, some elements show an unclear relationship between the geochemical element content and grain size, suggesting that the geochemical composition of sediments can be influenced by other factors (e.g. sources, sedimentary dynamics; Sanchez-Garcia et al., 2010; Zhao et al., 2019; Tursun et al., 2022). Therefore, it is challenging and potentially inaccurate to assess the sedimentary environmental evolution with a single geochemical element proxy. Additional, grain size as an indicator of environmental conditions also presents numerous changes (e.g. sediment sources, the variability of transport processes, and the sedimentary environments). This indicate that grain size parameters can only serve as a rough indicator of sedimentary environment changes (Meng et al., 2023). However, grain size end-member model facilitated the mathematical decomposition of the complete set of grain size data based on sedimentary dynamics and transport modes, enabling the extraction of dynamic information from each end-member and the elucidation of its environmental implications (Liu et al., 2021). The Yellow River estuary was a weakly tidal estuary dominated by river dynamics, formed by the injection of Yellow River sediment into a weakly tidal, weakly wave-powered marine environment. Its complex depositional environment was typical. The dynamic geomorphology and sedimentary environment of the estuary were complex. Therefore, it was important to investigate the evolution of the sedimentary environment of the Yellow River estuary and its response to the variability of incoming seawater sands, which can provide a reference for the study of other weakly tidal estuaries. It can also establish a knowledge link for the understanding of different types of estuaries. To enhance the precision of sedimentary environment determination, it was advisable to integrate sediment geochemical elements with grain size end-member results. In this study, we collected two cores YDC and YDG from the modern YRD, and investigated the distribution characteristics of grain size and chemical elements in modern sediments of the Yellow River Delta (YRD) region to reveal the sediment records in response to frequent estuarine channel migration and complex sedimentary environment.

## 2 Study area

The YRD (118°05'-119°10'E, 37°14'-38°10'N) is geographically defined by its borders with the Bohai Bay to the north and the Laizhou Bay to the east (Figure 1). Since 1855, Yellow River northward to the Bohai Sea, the modern YRD has been formed through the rapid deposition of significant amounts of sediment delivered by frequent shifting of the river's channel. According to the statistical data from Lijin Hydrology Station in the Yellow River mouth, the average annual water discharge is  $300.56 \times 10^8$  m<sup>3</sup>/yr and the average annual sediment load is  $6.88 \times 10^8$  t/yr (Fu et al., 2021). Recently, the Yellow River have experienced rapid reduction of sediment supply into the sea owing to extensive human activities such as water resource development, reservoir construction and water-sand diversion. The YRD is distinguished by a silty tidal flat that undergoes regular cycles of siltation and erosion as a result of sediment deposition and oceanic hydrodynamics. Wave patterns in the YRD are primarily

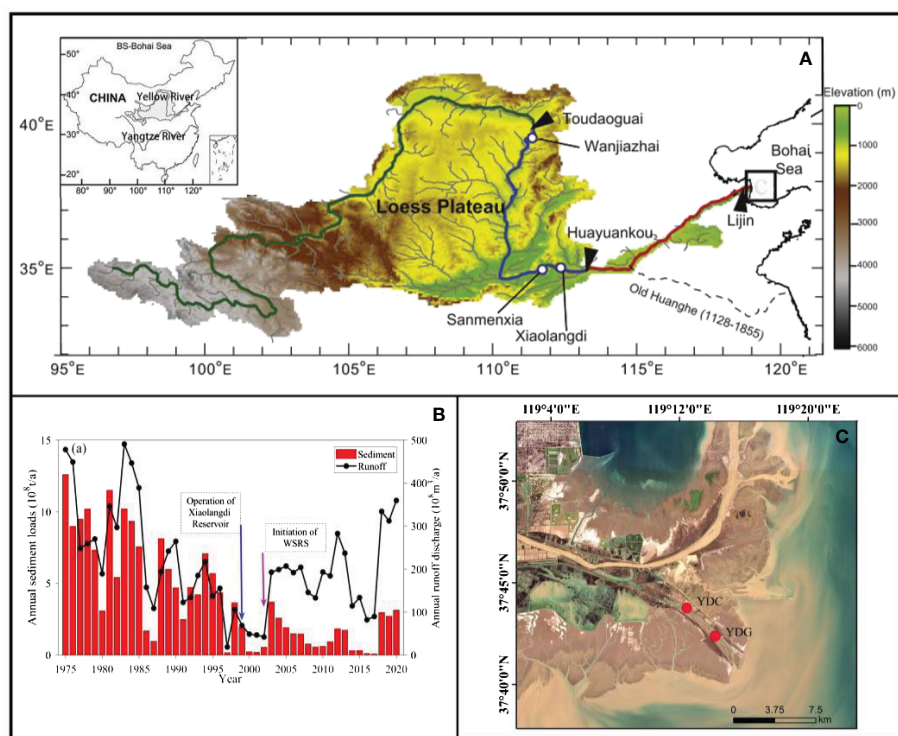


FIGURE 1

(A) Map of the Yellow River basin (Wu et al., 2017). (B) Interannual variations of sediment and water discharge a from 1975 to 2020 at Lijin station (Wang et al., 2022). (C) Map of river channel changes and core locations in the Yellow River delta.

influenced by the winds from the Bohai Sea, exhibiting significant seasonal variability in both direction and speed (Wang et al., 2022). The tidal regime of the YRD is dominated by an irregular semi-diurnal tide. The nearshore tidal range in the YRD is comparatively restricted, suggesting a reduced impact from tidal forces (Fu et al., 2021). The YRD region exhibits a warm-temperate semi-humid continental monsoon climate, displaying uniform climatic patterns in its northern and southern areas. The average annual temperature in the YRD ranges from 11.7°C to 12.8°C. The majority of precipitation occurs during the summer, contributing to 70% of the total annual rainfall, while average annual evaporation rates range from 1,900 to 2,400 mm.

### 3 Materials and methods

In 2018, cores YDC (119°11'17.03"E, 37°44'37.88"N) and YDG (119°11'20.01"E, 37°44'26.35"N) of 1m length were collected near the southern part of the Qing 8 course mouth in the modern YRD (Figure 1). The water depth of core sites was about 1.5 m. Subsequently, the cores were sectioned at 2 cm intervals, and a total of 50 samples were obtained from the cores YDC and YDG, respectively. Grain size samples smaller than 2 mm were analyzed using a Mastersizer 3000 laser grain sizer, which has a measuring range of 0.01–3000 μm with a measuring error of ≤0.02 μm. To ensure the accuracy of the experimental data, each sample was measured 3 times to take the average value. The Udden-Wentworth isobaric system,

which utilizes  $\Phi$ -values to classify grain sizes as <4 μm (clay), 4–63 μm (silt) and >63 μm (sand), was employed as the standard for grain size classification. The geochemical samples were analyzed at the Shaanxi Key Laboratory of Earth Surface System and Environmental Carrying Capacity, School of Urban and Environmental Sciences, Northwest University. The geochemical elemental analyses were conducted using a PW2403 X-Ray fluorescence spectrometer. The test items included the detection of major element such as SiO<sub>2</sub>, Fe<sub>2</sub>O<sub>3</sub>, CaO and K<sub>2</sub>O, and trace elements including Cl, Cu, Mn, Zn, Ga, Ba and Rb. Standard samples (GSS1, GSD12) were added for calibration during the measurement. The detection methods adhered to the Technical Regulations, GB/T14506-93 and DZG20.03-1987. The discrepancies between measured and reference values were found that within a margin of error of less than 5%. The test results satisfied the stipulated criteria in the Technical Specification. Further analyses, including correlation and principal factor analyses, were conducted on the standardized data units by using SPSS software.

## 4 Results and analysis

### 4.1 Grain-size characteristics

The results of the modern YRD sediment grain size analysis show that both cores YDC and YDG were primarily composed of clay and silt (Figure 2). The two cores were both divided into two units according to sedimentary characteristics. Within Unit 1 (28–

100 cm) of core YDC, the range of clay content exhibited the greatest variability with a maximum value of 79.26%. Conversely, in core YDG Unit 1 (28–100 cm), the clay content displayed the largest amplitude of variation peaking at 92.18%. In Unit 2 (0–28 cm) of core YDC, a maximum value of the silt content was 50.76%, and the maximum sand content was 15.98%. In Unit 2 of core YDG, the maximum clay value was 64.76%. The sediment grain-size composition and profiles of the two cores showed contrary trends. In core YDC, the clay content increased gradually from top to bottom with depth, and had higher content at the depth of Unit 1 (28–100 cm). While the silt and sand content showed a decreased trend from top to bottom, and both have higher content in Unit 2 (0–28 cm). In the core YDG, the higher clay content was mainly concentrated in Unit 2 (0–28 cm), while the silt and sand contents were highest in Unit 1 (28–100 cm). The variation of sediment characteristics within different cores indicates distinct sedimentary environments.

The average grain size of core YDC ranged from 0.28  $\mu\text{m}$  to 32.17  $\mu\text{m}$  with a mean value of 10.42  $\mu\text{m}$ . While core YDG average grain size exhibited a range of 0.08  $\mu\text{m}$  to 35.64  $\mu\text{m}$  with an average of 21.71  $\mu\text{m}$ , which showed a relatively narrow fluctuation range. The sorting coefficient ( $\sigma$ ) values of cores YDC and YDG ranged from 1.57 to 4.1 and 2.21 to 18.89, respectively, indicating relatively poor sorting. The skewness (Sk) values of core YDC exhibited a range from -0.62 to 0.56, while the core YDG displayed range from -0.63 to 0.58. The kurtosis (Kg) values of core YDC ranged from 0.57 to 1.56, while the core YDG ranged from 0.58 to 1.88, indicating a narrow kurtosis curve in both cores.

## 4.2 Characteristics of sediment geochemical elements

The chemical compositions of sediments served as proxy of variations in sediment sources, sedimentary environments, and

sedimentary dynamics (Li et al., 2021; Li et al., 2022; Li et al., 2023a; Liang and Jiang, 2017; Yang et al., 2021; Wei et al., 2023). An overwhelming presence of the major element  $\text{SiO}_2$  was identified in cores YDC and YDG (Table 1), with  $\text{SiO}_2$  content ranging from 49.25% to 61.16% (mean of 55.53%) in core YDC and from 45.99% to 62.96% (mean of 58.45%) in core YDG. The coefficients of variation for  $\text{SiO}_2$  content were calculated as 6.73% for core YDC and 7.58% for core YDG. The coefficient of variation for the  $\text{SiO}_2$  content in the two cores was found to be smaller. This similarly change was also observed from CaO, with content ranging from 6.34% to 8.14% (YDC) and 5.79% to 9.27% (YDG), respectively, which accompanied by small coefficients of variation. The  $\text{Fe}_2\text{O}_3$  content in cores YDC and YDG ranged from 3.6% to 5.4% and 3.33% to 5.98%, respectively.  $\text{K}_2\text{O}$  was identified as the lowest major element content, with average content of 2.25% and 2.23% in the two cores, respectively. The trace element composition of cores YDC and YDG was found to be both primarily composed of Cl, Mn and Ba. The average content of Cl was 18,462.8 mg/kg and 12,535.1 mg/kg, respectively. The coefficients of variation for elements were significantly high for the two cores YDC (54.06) and YDG (102.5), indicating a significant degree of variability between the two cores. In contrast, the contents of trace elements such as Cu, Mn, Zn, Ga, Ba and Rb do not exhibited significant changes overall, and coefficients of variation that were comparatively low.

The vertical changes of elemental composition with depth in the two cores were shown in Figures 3 and 4. The examination of geochemical elemental composition with the various grain sizes in sediment samples extracted from core YDC indicated three discernible patterns: a reduction in  $\text{SiO}_2$  and Ba, stabilization in Ga, Cu, and  $\text{K}_2\text{O}$ , and an elevation in Zn, Rb,  $\text{Fe}_2\text{O}_3$ , CaO, Mn, and Cl. Specifically, the CaO content increased from 6.34% in the surface to 8.14% in the bottom, and similar increasing trends were observed from Zn, Rb,  $\text{Fe}_2\text{O}_3$  and Mn. Furthermore, certain elements ( $\text{SiO}_2$  and Ba) exhibited a declining trend with increasing depth. The highest contents of Zn, Rb,  $\text{Fe}_2\text{O}_3$ , CaO, Mn and Cl were

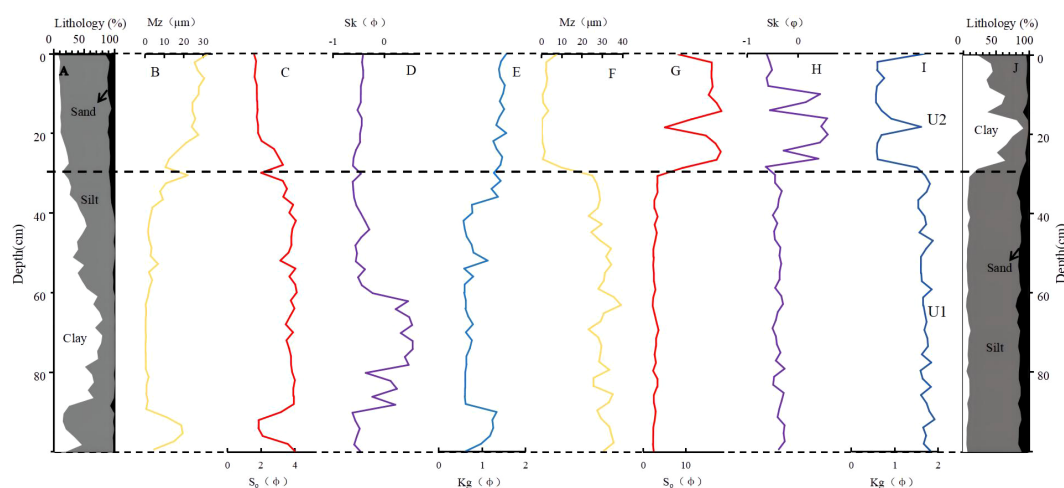


FIGURE 2 Characteristics of grain-size parameters with depth for cores YDC (A–E) and YDG (F–J).

TABLE 1 Major (weight percentage) and trace (ppm) elemental data for YDC and YDG cores.

	YDC				YDG			
	Max	Min	Mean	CV	Max	Min	Mean	CV
SiO <sub>2</sub>	61.16	49.25	55.53	6.73	62.96	45.99	58.45	7.58
K <sub>2</sub> O	2.45	2.02	2.25	5.45	2.56	2.1	2.23	5.07
CaO	8.14	6.34	7.18	6.97	9.27	5.79	6.68	12.13
Fe <sub>2</sub> O <sub>3</sub>	5.4	3.6	4.48	11.25	5.98	3.33	4.12	15.33
Cl	42319	5446	18462.8	54.06	53742	4151	12535.1	102.5
Mn	896	478	635.6	18.97	912	367	540.16	21.57
Cu	30	17	23.62	17.17	36	18	22.54	20.75
Zn	82	52	66.38	13.4	92	52	63.06	17.41
Ga	18	12	15.26	10.23	20	13	15.04	10.14
Ba	677	457	566.9	12.24	676	387	588.14	11.25
Rb	15.75	10.15	12.91	10.56	16.95	9.42	11.76	11.43

Trace element content in  $\times 10^{-6}$ .

all found in Unit 1 (0-28cm), indicating significant variability in elemental composition. The Cl contents fluctuate significantly was especially, which ranges from 4151 mg/kg to 53742 mg/kg with an average concentration of 12535.1 mg/kg. In contrast, the concentrations of Zn, Rb, Fe<sub>2</sub>O<sub>3</sub>, CaO, and Mn of core YDC exhibited a gradual decrease trend, and have higher concentration in Unit 2 (0-28cm) with relatively minor fluctuations in elemental content. The core YDC exhibited the most significant elemental variation within Unit 2 (28-100 cm), ranging from between 533 mg/kg and 866 mg/kg. Conversely, the fundamental changes in core YDG were small, exhibiting an opposite distribution trend with core YDC. Core YDG demonstrated significant elemental variations in Unit 1 (0-28 cm), while core YDC showed more pronounced differences in elemental composition in Unit 2 (28-100 cm).

## 5 Discussion

### 5.1 Geochemical environmental analysis

Geochemical elements were served as a significant indicator of sediment composition, and the observed variations of the geochemical elements can provide valuable information for the origins of sedimentary environments (Li et al., 2012; Zhang et al., 2013; Liu et al., 2016; Gao et al., 2021; Yuan et al., 2022). Meng et al. (2023) utilized the grain-size end-member analysis of the cores YDC and YDG to identify distinct end members (EM1, EM2, EM3, and EM4) associated with particular sedimentary processes (Table 2). The utilization of the geochemical characteristics and grain size distribution analysis demonstrated greater efficacy in

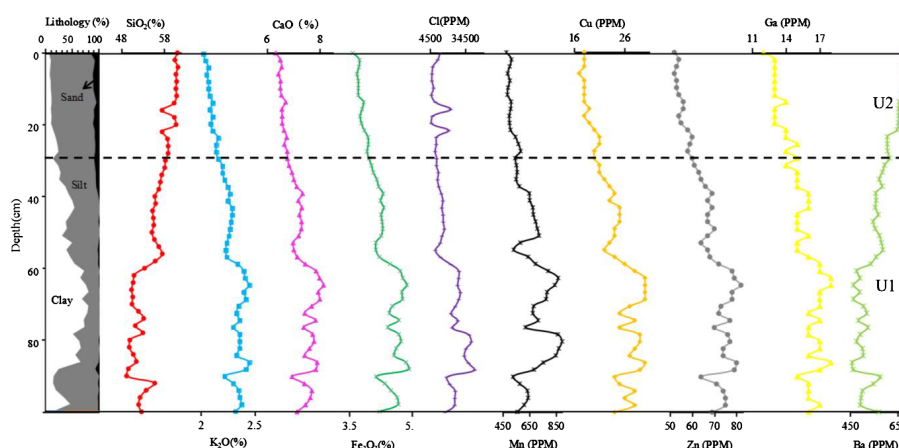


FIGURE 3 Characteristics of elemental content with depth for the YDC core.

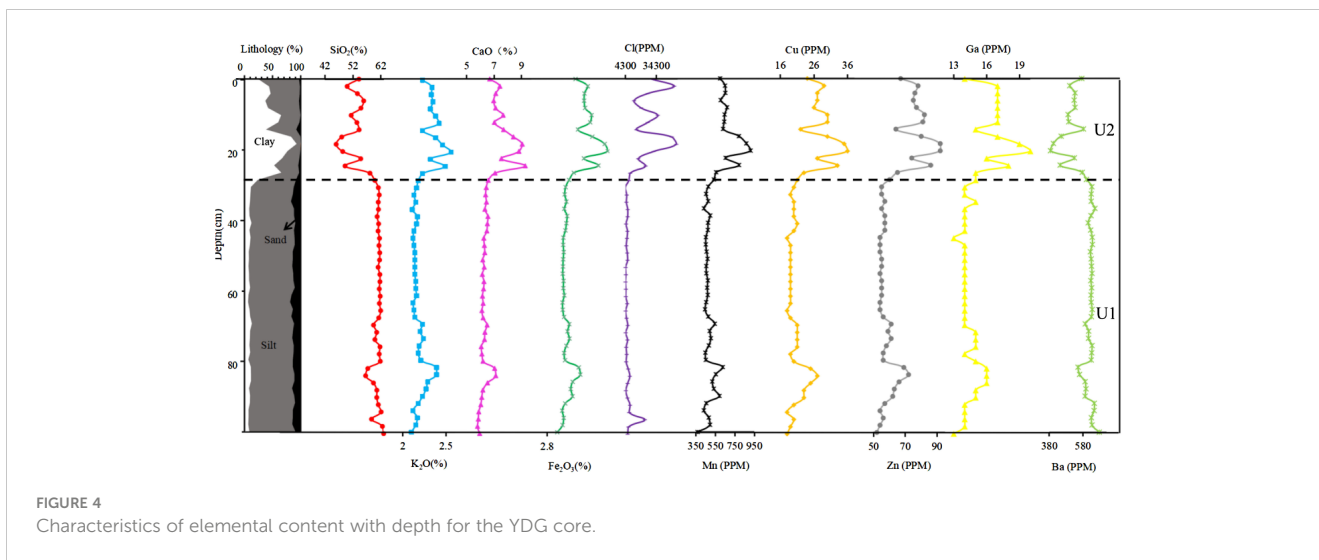


FIGURE 4 Characteristics of elemental content with depth for the YDG core.

identifying sediment sources and elucidating sedimentary environment evolution. Correlation analysis and R-mode cluster analysis were conducted on sediment grain-size end-members and chemical elements of cores YDC and YDG to effectively determine environmental significance of geochemical elements.

Meng et al. (2023) observed that EM1 and EM2 were characterized by the fine-grained sediment including clay and silt that were deposited under weak hydrodynamic conditions resulting from the long-distance sediment transport from the Yellow River. EM3 and EM4 consisted of coarse-grained sediments, such as coarse silt and sand, that were deposited under intense hydrodynamic conditions that were impacted by nearshore waves and tides. By analyzing the relationships between the four major

elemental compounds, the results showed that EM1 and EM2 exhibited negative correlations with SiO<sub>2</sub> ( $R^2=-0.83$ ,  $R^2=-0.62$ ) and significant positive correlations with K<sub>2</sub>O ( $R^2=0.746$ ,  $R^2=-0.62$ ), CaO ( $R^2=0.82$ ,  $R^2=-0.62$ ) and Fe<sub>2</sub>O<sub>3</sub> ( $R^2=0.84$ ,  $R^2=-0.62$ ). Conversely, EM3 and EM4 displayed positive correlations with SiO<sub>2</sub> ( $R^2=0.14$ ,  $R^2=-0.84$ ) and negative correlations with K<sub>2</sub>O ( $R^2=-0.27$ ,  $R^2=-0.64$ ), CaO ( $R^2=-0.18$ ,  $R^2=-0.81$ ) and Fe<sub>2</sub>O<sub>3</sub> ( $R^2=-0.62$ ,  $R^2=-0.83$ ). Among the eight trace elements, EM1 and EM2 were positively correlated with Cl ( $R^2=0.75$ ,  $R^2=-0.43$ ), Mn ( $R^2=0.83$ ,  $R^2=0.62$ ), Cu ( $R^2=0.81$ ,  $R^2=0.50$ ), Zn ( $R^2=0.83$ ,  $R^2=0.57$ ), Ga ( $R^2=0.79$ ,  $R^2=0.48$ ) and Rb ( $R^2=0.78$ ,  $R^2=-0.58$ ) and significantly negatively correlated with Ba ( $R^2=-0.83$ ,  $R^2=-0.54$ ). EM3 and EM4 were negatively correlated with Cl ( $R^2=-0.10$ ,  $R^2=-0.72$ ), Mn ( $R^2=-$

TABLE 2 Correlation analysis of each grain-size end member with geochemical elements of cores YDC and YDG.

	EM 1	EM 2	EM 3	EM 4	SiO <sub>2</sub>	K <sub>2</sub> O	CaO	Fe <sub>2</sub> O <sub>3</sub>	Cl	Mn	Cu	Zn	Ga	Rb	Ba
EM 1	1														
EM 2	0.45	1													
EM 3	-0.44	0.12	1												
EM 4	-0.78	-0.80	-0.15	1											
SiO <sub>2</sub>	-0.83	-0.62	0.14	0.84	1										
K <sub>2</sub> O	0.76	0.50	-0.27	-0.68	-0.89	1									
CaO	0.82	0.62	-0.18	-0.81	-0.94	0.84	1								
Fe <sub>2</sub> O <sub>3</sub>	0.84	0.62	-0.17	-0.83	-0.97	0.94	0.95	1							
Cl	0.75	0.43	-0.10	-0.72	-0.93	0.74	0.80	0.85	1						
Mn	0.83	0.62	-0.23	-0.80	-0.92	0.84	0.90	0.92	0.81	1					
Cu	0.81	0.50	-0.21	-0.75	-0.94	0.97	0.90	0.97	0.83	0.89	1				
Zn	0.83	0.57	-0.19	-0.80	-0.95	0.96	0.91	0.98	0.83	0.89	0.99	1			
Ga	0.79	0.48	-0.29	-0.69	-0.87	0.95	0.84	0.92	0.74	0.84	0.95	0.94	1		
Rb	0.78	0.55	-0.15	-0.77	-0.93	0.95	0.82	0.94	0.85	0.85	0.96	0.97	0.92	1	
Ba	-0.84	-0.54	0.27	0.76	0.95	-0.96	-0.91	-0.97	-0.83	-0.90	-0.97	-0.97	-0.94	-0.95	1

0.23,  $R^2=-0.80$ ), Cu ( $R^2=-0.21$ ,  $R^2=-0.75$ ), Zn ( $R^2=-0.19$ ,  $R^2=-0.77$ ), Ga ( $R^2=-0.29$ ,  $R^2=-0.69$ ) and Rb ( $R^2=-0.15$ ,  $R^2=-0.77$ ) and positively correlated with Ba ( $R^2=0.27$ ,  $R^2=0.76$ ). Generally, the reaction for sedimentary dynamic conditions exhibited greater intensity when the sediment grain size is coarser. Variations of sediment composition caused by fluctuations of hydrodynamic conditions can result in the differences of elemental contents (Lucic et al., 2021). The results indicated that the content of  $\text{SiO}_2$  and Ba were influenced by grain size with the enrichment decreasing as grain size increases, which suggested a predominance of coarse minerals that exhibited greater resistance to weathering. The contents of  $\text{K}_2\text{O}$ , CaO,  $\text{Fe}_2\text{O}_3$ , Cl, Mn, Cu, Zn, Ga and Rb were also clearly controlled by grain size. Their enrichment increased with decreasing sediment grain size. This suggested that the primary minerals containing these elements exhibited limited resistance to weathering, rendering them susceptible to fragmentation or erosion into clay-like minerals (Li et al., 2016; Wang et al., 2019).

R-mode cluster analysis was a multivariate statistical method used to examine the relationships among chemical elements by analyzing the changes in the content of multiple elements and simplifying multivariate variables to univariate ones. The geochemical characteristics of sediments of the core YRD were affected by various factors including sediment sources and sedimentary environments. The chemical fractions of sediments from two cores can be classified into three distinct elemental assemblages (Figure 5). The first group of assemblages included the major elements  $\text{K}_2\text{O}$ , CaO,  $\text{Fe}_2\text{O}_3$  and the trace elements Mn, Cu, Zn, Ga, Rb, which showed susceptibility to redox effects and a sensitive environmental response. Specifically, CaO and Mn were the manifestations of the high calcium carbonate content in the sediments of the Yellow River source, which was easy to oxidize to generate carbonate and reflects the changes of the sedimentary environment. The second group of assemblages consisted of  $\text{SiO}_2$  and Ba, with the sediment elements being influenced by grain size. The third group exclusively contained Cl. The cores were located in

close proximity to the mouth of the Yellow River, subjected to the marine environment. Cl served as a marine controlling factor in the marine environment.

Geochemical analysis was performed to elucidate the origins and controlling factors of elements in the sediments of the two cores, providing insights into sedimentary processes and environmental changes. This analysis employed R-mode factor analysis using major and trace elements as variables. The results showed that sediment chemical composition was impacted by three factors leading to the classification of sediment elemental content (Table 3). These factors contributed variances of 45.08%, 28.53% and 23.77%, and the cumulative contribution of 97.38%. The chemical combinations of the elements associated with the  $F_1$  factor included  $\text{SiO}_2$ ,  $\text{K}_2\text{O}$ ,  $\text{Fe}_2\text{O}_3$ , Cu, Zn, Ba, Ga and Rb. The research revealed a significant positive relationship between  $\text{SiO}_2$  and the grain size, whereas Ba enrichment exhibited a negative correlation with the grain size. Because of the changes of the sedimentary environment,  $\text{K}_2\text{O}$  and  $\text{Fe}_2\text{O}_3$  exhibited a propensity to assume colloidal or granular states when sediments entered the ocean and were adsorbed by clay minerals (Wang and Yu, 2015). Rb was a stabilizing factor during the process of weathering and was mainly retained by adsorption from clay sediments (Wang and Yu, 2015). Therefore, it can be inferred that  $F_1$  was closely related to clay minerals and represented the control of the grain size. The  $F_2$  factor was represented by CaO, Mn,  $\text{SiO}_2$ . According to previous studies, the Yellow River was characterized by a significantly high Ca content (Zhao et al., 2016). Sediments from the Yellow River were rich in carbonates, facilitating the enrichment of Mn to form carbonates. The chemically stable mineral  $\text{SiO}_2$  was readily preserved in land-sourced detritus leading to a decrease in the content of other elements (Wang and Yu, 2015). This dilution effect of  $\text{SiO}_2$  was often negatively correlated with other elements. Analysis of chemical element correlations suggests that  $F_2$  may serve as a controlling factor of the Yellow River (Table 3).  $F_3$  is characterized by the dominance of Cl, representing the chemical composition of seawater. In 1996, the diversion of the Yellow River to the Qing 8 course resulted in a change in the sediment source of two cores. The hydrodynamic influence of nearshore waves and tides strengthened ocean control. Therefore,  $F_3$  can be served as a marine control factor.

## 5.2 Significance of source indication of sediment chemical elements

The transportation of chemical elements in natural systems was distinguished by the prevalence of stable elements in water with brief residence times. Mechanical sedimentation occurred rapidly under appropriate hydrodynamic conditions without significant chemical changes (Wang and Yu, 2015; Gao et al., 2021). As a result, the chemical elements were transported in nearly equal proportions leading to a more precise depiction of sedimentary dynamics and environments. The examination of sediment chemical composition has been shown to be a valuable approach for studying the sources of sediment (Faust et al., 2014; Wang and Yu, 2015; Xiao et al., 2020). Meng et al. (2023) conducted a detailed

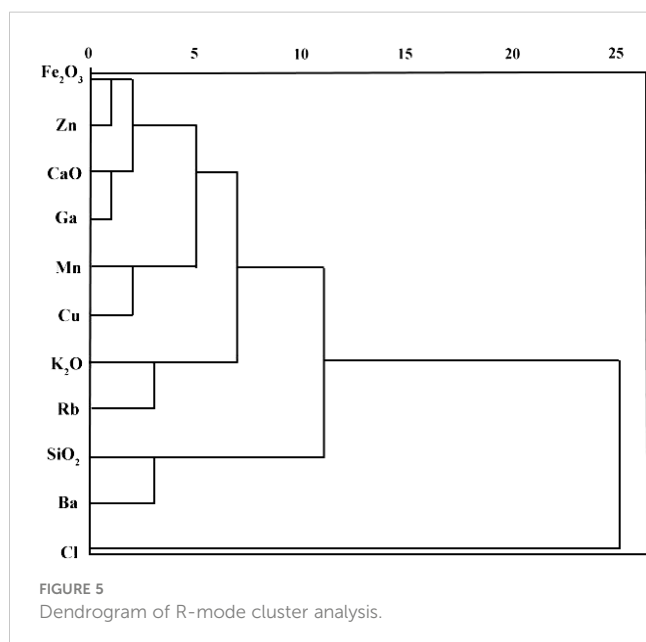


TABLE 3 R-mode rotating factor loadings for each element of YDC and YDG boreholes.

	$F_1$	$F_2$	$F_3$
K <sub>2</sub> O	0.844	0.412	0.314
CaO	0.485	0.765	0.378
Fe <sub>2</sub> O <sub>3</sub>	0.651	0.601	0.448
Cl	0.376	0.382	0.840
Cu	0.751	0.479	0.432
Zn	0.743	0.496	0.435
Ga	0.828	0.421	0.302
Rb	0.765	0.348	0.521
SiO <sub>2</sub>	-0.739	-0.583	-0.399
Mn	0.487	0.713	0.423
Ba	-0.731	-0.502	-0.437
Cumulative contribution rate	45.09	73.62	97.39

analysis of the sediment characteristics and grain-size end-members data from cores YDC and YDG, which were subsequently divided into two distinct units: Unit 1 (28-100 cm) and Unit 2 (0-28 cm). Based on the abrupt change in sediment grain size and end member

data at 28 cm, and in combination with the sediment sedimentary rate, it was deduced that 28-100 cm was formed before 1996, and 0-28 cm was formed after the Yellow River was diverted (1996-2018). The sedimentary environments of cores YDC and YDG exhibited dynamic changes due to alterations in river channels and anthropogenic influences. Core YDC was located in the delta-plain sedimentary facies, and core YDG was located in the delta-front facies (Meng et al., 2023).

Unit 1 (28-100 cm) was formed before the Yellow River was diverted to the Qing 8 course in 1996. The sediment in the two cores primarily source from the Yellow River and consists mainly of sandy clay (Figure 6) (Shi, 2021; Meng et al., 2023). The sedimentary environment was characterized by siltation. The Yellow River sediments contain CaO, a representative content in the erosion processes of the Loess Plateau. Additionally, the loess sediments transported by the river also impacted its chemical composition. The sediments from the Yellow River exhibited high carbonate content with the element Mn readily enriching to form carbonates. The average content of CaO was 7.44% in the core YDC and 6.27% in the core YDG, and the average content of Mn was 687.97 mg/kg and 480.14 mg/kg, respectively. The sedimentary environment was primarily influenced by the Yellow River.

In addition, the distinct sedimentary phases of the two cores resulted in significant differences of their chemical compositions. Specifically, the delta-front facies exhibited a lower clay content and higher sand content compared with the incoming sand, while the

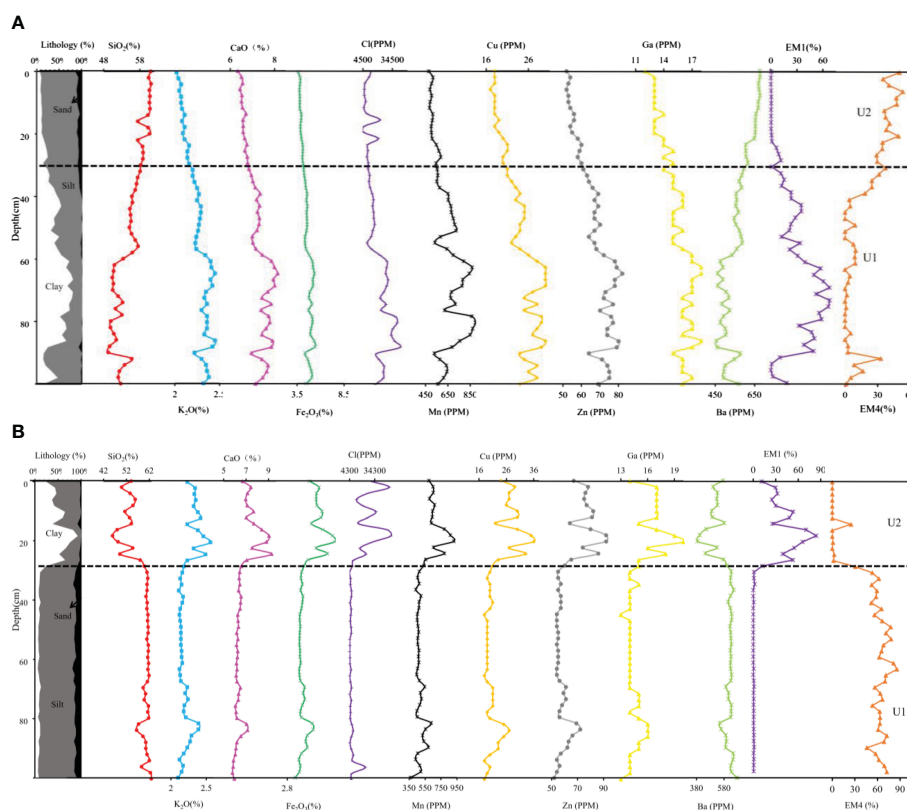


FIGURE 6 Comprehensive diagram of cores YDC (A) and YDG (B), including lithological characteristics of the study section, depth profiles of each element, and representative end-member depth profiles.



silt content remained relatively consistent. The clay content of the core YDG located in the delta-front facies was measured at 8.4%, which was significantly lower than the 46.8% clay content observed in core YDC. The sand content of 13.73% was higher than that of 2.49% in the core YDC. The results of chemical element analyses showed that SiO<sub>2</sub> was identified as a characteristic element of sands due to its predominant enrichment in sandy sediments and coarse-grained composition in accordance with the grain size control law of elements. The SiO<sub>2</sub> content demonstrated a gradual increase with larger grain sizes. In Unit 1 (28–100 cm), cores YDG and YDC exhibited average contents of SiO<sub>2</sub> are 63.88% and 53.65%, respectively, and Ba contents of 622.49 mg/kg and 530.03 mg/kg. The two cores were located an estuarine region influenced by the interaction of river and ocean dynamics resulting in a diverse sedimentary environment characterized by alternating processes of river siltation, wave and tidal erosion. Wu et al. (2017) demonstrated the significant impact of river flow and sediment grain size on the evolution of the delta. Before 1996, the implementation of engineering interventions led to the channelization of the river causing an increase of the suspended sand grain size at the inlet. The gradual seaward advancement of the active delta at a rate of 11.9 km<sup>2</sup>/yr. The dominant sediment types of the core YDG were silt and sand with an average silt content of 77.8%, while the core YDC was characterized by clay and silt with a relatively high clay content of 46.8%. The coarse-grained fraction EM4 in core YDG had an average content of 66.5%, while the fine-grained fraction EM1 in core YDC averaged 33.75%. The sediment grain-size compositions of the two cores were reflect the variations between them. Sediments from the Yellow River source spread to the distant sea after the fine particles are resuspended by wave action. Therefore, the sediments in this area were mainly fine particles, which were easy to adsorb chemical elements. Additionally, the elemental compositions of the cores correlated with the variations of the sediment grain-size composition. The analysis of chemical elements distribution with depth revealed that the trends of major elements K<sub>2</sub>O, Fe<sub>2</sub>O<sub>3</sub> and trace elements Cu, Zn, Ga, Rb, which were adsorbed from clay sediments, exhibited variations based on the granularity of the sediment particles.

Unit 2 (0–28 cm) was formed during 1996–2018. The Yellow River was artificially diverted in 1996. The entrance to the sea extended from the Qing 8 course to the northeast and eroded to the southeast. The sedimentary dynamics of the two cores changed from siltation to erosion as results of alterations in topography, geomorphology, sediment sources and river-sea interactions (Meng et al., 2023). The change in the sedimentary source of the Yellow River resulted in a decrease in the content of fine-grained sediments including clay and silt. The grain size of the core YDC exhibited a favorable response for the change of the sedimentary source. In Unit 2 (0–28 cm), there was a notable increase of the silt and sand content by 28.6% and 80%, respectively, while the clay content decreased by 35.4%. The EM1 content exhibited a rapid decrease to an average of 1.3%, and the EM4 content experienced a significant increase to 40.2%. The strong hydrodynamic forces from clockwise circulation and coastal currents resulted in the recurrent scouring of sediments, which showed fine-grained sediment to be transported away and coarser-grained sediment to be deposited. The core YDC

was in a hydrodynamic environment characterized by coarser sediments with lower adsorption capacity for chemical elements resulting in a low content of chemical elements. Analysis of sediment chemical elements indicated a reduction in the average content of CaO as a key indicator of the Yellow River source. The average Mn content decreased to 513.27 mg/kg, while the average contents of SiO<sub>2</sub> and Ba influenced by grain size increased to 60% and 653 mg/kg, respectively. Core YDG, located in the delta-front facies, is subject to heightened impacts from tidal currents and marine wave action, which lead to a significant sedimentary effect from the diffusion of nearshore fine sandy clay suspension (Han et al., 2011; Zhou et al., 2016; Shi, 2021). This was evidenced by a rapid increase of the clay content by 85% in Unit 1 compared with Unit 2 and a significant increase of the EM1 content by an average of 44.5%. Additionally, reductions of the silt and sand content were observed with the most notable decrease of 96% in sand content. The EM4 content was reduced accordingly with an average content of 2.2%. Owing to the influences of the finer grain-size composition of the sediments, there was a reduction in the average content of SiO<sub>2</sub> and Ba by 15% and 43%, respectively. The profiles of major elements K<sub>2</sub>O, Fe<sub>2</sub>O<sub>3</sub> and trace elements Cu, Zn, Ga, Rb exhibited a same trend of variation with clay content with average contents of 2.36%, 4.97%, 28.5 mg/kg, 77.78 mg/kg, 16.86 mg/kg and 109.57 mg/kg, respectively.

The core YRD was located in the coastal humid-semi-humid seawater-impregnated saline zone, a modern salt accumulation process (Fan et al., 2010). Coastal saline soils were formed through regular inundation and lateral impregnation by seawater, resulting in the accumulation of salt due to strong evaporation. Core YDG in the eastern part of the YRD was strongly impregnated by seawater via lateral seepage, and mineralization of the groundwater was relatively high (Li et al., 1998; Wu et al., 2017). These geochemical elements were significantly influenced by the return of salt from groundwater resulting in a significant increase of the salt accumulation in the surface layer compared to other regions. Cl was a primary component of seawater and served as a controlling factor in oceanic processes. The average content of Cl at Unit 2(0–28 cm) was 28566.21 mg/kg, which represented a fourfold increase compared to the content observed at Unit 1(28–100 cm). Core YDC was located the delta-plain sedimentary facies, where the effects of seawater infiltration were restricted and the influence of salt re-entry from groundwater was limited, resulting in a subsurface salinity distribution higher than that of the surface layer.

## 6 Conclusion

The sediment grain-size composition and geochemical elements of the cores YDC and YDG were analyzed through field collection of modern YRD core sediments combined with the sediment grain-size end member analysis method. This study offered valuable insights for understanding the evolution of sedimentary dynamics and the sedimentary environment in the modern YRD.

- (1) Significant differences were observed in the grain-size compositions of cores YDC and YDG with both cores

primarily consisting of silt and exhibiting a dispersed grain-size composition. In Unit 1 (28–100 cm), the average grain size of cores YDC and YDG were 4.96  $\mu\text{m}$  and 30.04  $\mu\text{m}$ , respectively with fine silt and medium silt being the main components. In Unit 2 (0–28 cm), the average grain size of cores YDC and YDG was 23.85  $\mu\text{m}$  and 2.25  $\mu\text{m}$ , respectively with silt and clay being the dominant grain sizes.

- (2) The results from the cluster analysis and factor analysis of sediment chemical elements in cores YDC and YDG indicated that the distribution of these elements was influenced by three factors including source, grain size and seawater. Specifically, CaO and Mn were identified as source-control elements, while  $\text{SiO}_2$ ,  $\text{K}_2\text{O}$ ,  $\text{Fe}_2\text{O}_3$ , Cu, Zn, Ba, Ga and Rb were associated with grain size control. Cl was identified as a control element for the marine environment.
- (3) The cores YDC and YDG in the modern YRD recorded the diversion of the river and the evolution of the sedimentary environment near the mouth of the Yellow River at the Qing 8 course. Based on the sediment grain size composition and grain size end member data, it was concluded that the core YDC was located in the delta-plain sedimentary facies, and the core YDG was located in the delta-front facies. Before the Yellow River was diverted to the Qing 8 course in 1996, cores YDC and YDG were in the delta-front estuarine sedimentary environment with a reference point of 28 cm. The clay and silt content exhibited higher levels with the CaO content serving as a key indicator of the source of the Yellow River showing a significant increase. Additionally, the  $\text{SiO}_2$  content as an indicator of the rate of grain size control decreased with finer grain size. The elemental Cl content of core YDC was significantly higher than that of core YDG owing to the influence of subsurface re-salting. After the diversion of the Yellow River to the Qing 8 course, the core YDC located in the delta-plain sedimentary facies exhibited a significant decrease in clay content alongside an elevation of the coarse-grained silt and sand content. The contents of  $\text{K}_2\text{O}$ ,  $\text{Fe}_2\text{O}_3$ , Cu and Zn elements decreased, whereas those of  $\text{SiO}_2$  and Ba increased. The rapid changes observed in core YDG including the increases of the clay content, CaO and Mn contents, and a decrease in  $\text{SiO}_2$  content can be attributed to the suspension and diffusion of nearshore fine sand influenced by tidal currents and wave. Influenced by seawater impregnation and subsurface re-salinization, the Cl content of the surface was much higher than that in other parts of the core. The sedimentary environment changed from river sedimentation to nearshore wave erosion.

## Data availability statement

The raw data supporting the conclusions of this article will be made available by the authors, without undue reservation.

## Author contributions

LM: Investigation, Methodology, Software, Writing – original draft. LW: Funding acquisition, Methodology, Writing – review & editing. QW: Funding acquisition, Writing – review & editing. JZ: Methodology, Writing – review & editing. GZ: Writing – review & editing. CZ: Investigation, Writing – review & editing. XL: Investigation, Writing – review & editing. BC: Writing – review & editing. LZ: Writing – review & editing.

## Funding

The author(s) declare financial support was received for the research, authorship, and/or publication of this article. This research was supported financially by National Natural Science Foundation of China (No. 42377207, 42330406), the Foundation of School and Land Integration Development in Yantai (NO. 2021XDRHXMQT18), the open foundation of State Key Laboratory of Lake Science and Environment (No. 2022SKL005), the open foundation of State Key Laboratory of Loess and Quaternary Geology, Institute of Earth Environment, CAS (NO. SKLLQG2024). Youth Innovation Team Project for Talent Introduction and Cultivation in Universities of Shandong Province.

## Conflict of interest

The authors declare that the research was conducted in the absence of any commercial or financial relationships that could be construed as a potential conflict of interest.

## Publisher's note

All claims expressed in this article are solely those of the authors and do not necessarily represent those of their affiliated organizations, or those of the publisher, the editors and the reviewers. Any product that may be evaluated in this article, or claim that may be made by its manufacturer, is not guaranteed or endorsed by the publisher.

## References

- Cai, G. Q., Li, S., Zhao, L., Gao, H. F., and Zhong, H. X. (2018). Geochemical characteristics of surface sediments from the middle deep-sea basin of South China Sea. *Mar. Geology Quaternary Geology* 38, 90–101. doi: 10.16562/j.cnki.0256-1492.2018.05.009
- Cao, M. (1992). Distribution of chemical elements in tide flat sediments on the northern shore of Hangzhou Bay. *Trans. Oceanology Limnology* 04), 25–31. doi: 10.13984/j.cnki.cn37-1141.1992.04.005

- Cui, X. J., Sun, H., Dong, Z. B., Li, J. Y., Gao, X. M., and Li, C. (2017). Geochemical elements composition of sediments for mega-dunes and its environmental significance in the badain jaran sand sea. *J. Desert Res.* 37, 17–25. doi: 10.7522/j.issn.1000-694X.2015.00204
- Dethier, E. N., Renshaw, C. E., and Magilligan, F. J. (2022). Rapid changes to global river suspended sediment flux by humans. *Science* 376, 1447–1452. doi: 10.1126/science.abc7980
- Fan, X. M., Liu, G. H., Tang, Z. P., and Shu, L. C. (2010). Analysis on main contributors influencing soil salinization of yellow river delta. *J. Soil Water Conserv.* 24, 139–144. doi: 10.13870/j.cnki.stbcbx.2010.01.030
- Faust, J. C., Knies, J., Slagstad, T., Vogt, C., Milzer, G., and Giraudeau, J. (2014). Geochemical composition of Trondheimsfjord surface sediments: Sources and spatial variability of marine and terrigenous components. *Continental Shelf Res.* 88, 61–71. doi: 10.1016/j.csr.2014.07.008
- Fu, Y. T., Chen, S. L., Ji, H. Y., Fan, Y. S., and Li, P. (2021). The modern Yellow River Delta in transition: Causes and implications. *Mar. Geology* 436, 106476. doi: 10.1016/j.margeo.2021.106476
- Gao, X. M., Qu, X., Wang, M., Zhang, S. Y., Zhang, Y. Y., and Li, J. Y. (2021). Composition of geochemical elements and its implications for long-ridge yardang in the northwestern Qaidam Basin, China. *J. Desert Res.* 41, 127–136. doi: 10.7522/j.issn.1000-694X.2021.00034
- Han, G., Li, Y., Yu, J., Xu, J. W., Wang, G. M., and Zhang, Z. D. (2011). Evolution process and related driving mechanisms of Yellow River Delta since the diversion of Yellow River. *Chin. J. Appl. Ecol.* 22, 467–472. doi: 10.13287/j.1001-9332.2011.0047
- Hou, C., Yi, Y., Song, J., and Zhou, Y. (2021). Effect of water-sediment regulation operation on sediment grain size and nutrient content in the lower Yellow River. *J. Cleaner Production* 279, 123533. doi: 10.1016/j.jclepro.2020.123533
- Jiang, C., Chen, S., Pan, S., Fan, Y. S., and Ji, H. Y. (2018). Geomorphic evolution of the Yellow River Delta: Quantification of basin-scale natural and anthropogenic impacts. *Catena* 163, 361–377. doi: 10.1016/j.catena.2017.12.041
- Li, B. F., Feng, Q., Li, Z. J., Wang, F., Yu, T. F., Guo, X. Y., et al. (2022). Geochemical characteristics of surface aeolian sand in the Badain Jaran Desert, northwestern China: Implications for weathering, sedimentary processes and provenance. *CATENA* 219, 106640. doi: 10.1016/j.catena.2022.106640
- Li, C. F., Wang, Z. C., Li, Z. W., Xu, X. L., and Wang, K. L. (2023a). Using geochemical elements to discriminate sediment sources in a typical karst watershed. *Soil Tillage Res.* 232, 105778. doi: 10.1016/j.still.2023.105778
- Li, C. L., Kang, S. C., Zhang, Q. G., and Gao, S. P. (2012). Geochemical evidence on the source regions of Tibetan Plateau dusts during non-monsoon period in 2008/09. *Atmospheric Environ.* 59, 382–388. doi: 10.1016/j.atmosenv.2012.06.006
- Li, G., Wei, H., Yue, S., Cheng, Y. J., and Han, Y. S. (1998). Sedimentation in the Yellow River delta, part II: suspended sediment dispersal and sedimentary on the subaqueous delta. *Mar. Geology* 149, 113–131. doi: 10.1016/S0025-3227(98)00032-2
- Li, Q. L., Qiao, S. Q., Shi, X. F., Hu, L. M., Chen, Y. F., Bai, Y. Z., et al. (2021). Sediment provenance of the East Siberian Arctic Shelf: Evidence from clay minerals and chemical elements. *Acta Oceanologica Sin.* 43, 76–89. doi: 10.12284/hyxb2021041
- Li, W. Q., Qian, H., Xu, P. P., Hou, K., Qu, W. A., Ren, W. H., et al. (2023b). Insights into mineralogical distribution mechanism and environmental significance from geochemical behavior of sediments in the Yellow River Basin, China. *Sci. Total Environ.* 903, 166278. doi: 10.1016/j.scitotenv.2023.166278
- Li, X. M., Yan, P., Wu, W., and Qian, Y. (2016). The spatial distribution difference of surface elements in the river-desert transition zone of three drainages in Northern China. *Acta Sedimentologica Sin.* 34, 615–625. doi: 10.14027/j.cnki.cjxb.2016.04.001
- Liang, L. J., and Jiang, H. C. (2017). Geochemical composition of the last deglacial lacustrine sediments in East Tibet and implications for provenance, weathering, and earthquake events. *Quaternary Int.* 430, 41–51. doi: 10.1016/j.quaint.2015.07.037
- Ling, Z. Y., Li, J. S., Jin, J. H., Wang, J. P., Kong, F. C., and Chen, L. (2021). Geochemical characteristics and provenance of aeolian sediments in the Yarlung Tsangpo valley, Southern Tibetan Plateau. *Environ. Earth Sci.* 80, doi: 10.1007/s12665-021-09928-5
- Liu, Y., Cheng, Q. M., Zhou, K. F., Xia, Q. L., and Wang, X. Q. (2016). Multivariate analysis for geochemical process identification using stream sediment geochemical data: A perspective from compositional data. *Geochemical J.* 50, 293–314. doi: 10.2343/geochemj.2.0415
- Liu, Z. Y., Gu, X., Lian, M. S., Wang, J., Xin, M., Wang, B. D., et al. (2023). Occurrence, geochemical characteristics, enrichment, and ecological risks of rare earth elements in sediments of “the Yellow river–Estuary–bay” system. *Environ. pollut.* 319, 121025. doi: 10.1016/j.envpol.2023.121025
- Liu, L., Wang, H. J., Yang, Z. S., Fan, Y. Y., Wu, X., Hu, L. M., et al. (2022). Coarsening of sediments from the Huanghe (Yellow River) delta-coast and its environmental implications. *Geomorphology* 401, 108105. doi: 10.1016/j.geomorph.2021.108105
- Liu, R., Yue, D., Zhao, J., Su, Z. S., Shi, H., and Wang, X. Y. (2021). Characteristics of grain size end members and its environmental significance of aeolian sand/loess sedimentary sequence since L2 in Hengshan, Shaanxi Province. *Arid Land Geogr.* 44, 1328–1338. doi: 10.12118/j.issn.1000-6060.2021.05.14
- Lucic, M., Mikac, N., Bacic, N., and Vdovic, N. (2021). Appraisal of geochemical composition and hydrodynamic sorting of the river suspended material: Application of time-integrated suspended sediment sampler in a medium-sized river (the Sava River catchment). *J. Of Hydrology* 597. doi: 10.1016/j.jhydrol.2020.125768
- Meng, L. W., Wang, L. S., Zhao, J. W., Zhan, C., Liu, X. B., et al. (2023). End-member characteristics of sediment grain size in modern Yellow River delta sediments and its environmental significance. *Front. Mar. Sci.* 10. doi: 10.3389/fmars.2023.1141187
- Milliman, J. D., and Meade, R. H. (1983). World-wide delivery of river sediment to the oceans. *J. Geology* 91, 1–21. doi: 10.1086/628741
- Pang, H. L., Gao, H. S., Li, F. Q., and Zhang, L. K. (2022). Geochemical element composition and spatial distribution characteristics of sediments in the Ningxia-Inner Mongolia section of the Yellow River. *J. Desert Res.* 42, 44–53. doi: 10.7522/j.issn.1000-694X.2022.00012
- Sanchez-Garcia, L., de Andres, J. R., and Martin-Rubi, J. A. (2010). Geochemical signature in off-shore sediments from the Gulf of Cadiz inner shelf Sources and spatial variability of major and trace elements. *J. Mar. Syst.* 80, 191–202. doi: 10.1016/j.jmarsys.2009.10.009
- Shi, Z. X. (2021). Sedimentary and dispersal of different grain-size sediments in the Yellow River estuary. *Geographical Res.* 40, 1125–1133. doi: 10.11821/dlyj020200203
- Tursun, D., Zhang, F., Wu, F., Liu, X. F., Wu, S. X., Sun, T., et al. (2022). Geochemical characterization of major elements in Gurbantunggut Desert sediments, northwestern China and their regional variations. *Aeolian Res.* 57. doi: 10.1016/j.aeolia.2022.100802
- Wang, H., Bi, N., Saito, Y., Wang, Y., Sun, X. X., Zhang, J., et al. (2010). Recent changes in sediment delivery by the Huanghe (Yellow River) to the sea: Causes and environmental implications in its estuary. *J. Hydrology* 391, 302–313. doi: 10.1016/j.jhydrol.2010.07.030
- Wang, J. J., Shi, B., Yuan, Q. Y., Zhao, E. J., Bai, T., and Yang, S. P. (2022). Hydro-morphological regime of the lower Yellow river and delta in response to the water-sediment regulation scheme: Process, mechanism and implication. *CATENA* 219, 106646. doi: 10.1016/j.catena.2022.106646
- Wang, Y. J., Wu, F. D., and Li, X. M. (2019). Geochemical features of macro elements in Yardang sediments in Dunhuang and the indicative meanings. *J. Arid Land Resour. Environ.* 33, 161–167. doi: 10.13448/j.cnki.jalre.2019.122
- Wang, Z. D., and Yu, D. S. (2015). Analysis on the grain size and the geochemical characteristics of surface sediments in Quanzhou Bay. *J. Appl. Oceanography* 34, 568–579. doi: 10.3969/J.ISSN.2095-4972.2015.04.016
- Wei, G. R., Zhang, C. L., Li, Q., Wang, H. T., Wang, R. D., Zhang, Y. J., et al. (2023). Characterization of geochemical elements in surface sediments from Chinese deserts. *Catena* 220, 106637. doi: 10.1016/j.catena.2022.106637
- Wu, X., Bi, N. S., Xu, J. P., et al. (2017). Stepwise morphological evolution of the active Yellow River (Huanghe) delta lobe, (1976–2013): Dominant roles of riverine discharge and sediment grain size. *Geomorphology Amsterdam* 292, 115–127. doi: 10.1016/j.geomorph.2017.04.042
- Wu, X., Wang, H., Bi, N., Nittrouer, J. A., Xu, J. P., Cong, S., et al. (2020). Evolution of a tide-dominated abandoned channel: A case of the abandoned Qingshuigou course, Yellow River. *Mar. Geology* 422, 106116. doi: 10.1016/j.margeo.2020.106116
- Xiao, C. H., Wang, Y. H., Tian, J. W., Wang, X. C., and Xin, Y. (2020). Mineral composition and geochemical characteristics of sinking particles in the Challenger Deep, Mariana Trench: Implications for provenance and sedimentary environment. *Deep-Sea Res. Part I-Oceanographic Res. Papers* 157. doi: 10.1016/j.dsr.2019.103211
- Xu, J. (2000). Grain-size characteristics of suspended sediment in the Yellow River, China. *Catena* 38, 243–263. doi: 10.1016/S0341-8162(99)00070-3
- Yang, S. L., Luo, Y. L., Li, Q., Liu, W. M., Chen, Z. X., Liu, L., et al. (2021). Comparisons of topsoil geochemical elements from Northwest China and eastern Tibetan Plateau identify the plateau interior as Tibetan dust source. *Sci. total Environ.* 798. doi: 10.1016/j.scitotenv.2021.149240
- Yuan, Y., Liu, B. L., and Liu, H. (2022). Geochemical characteristics of sediments from East Dongting Lake and their implications for provenance and weathering. *Geosciences J.* 26, 335–348. doi: 10.1007/s12303-021-0040-4
- Zhang, W. X., Shi, Z. T., Chen, G. J., Liu, Y., Niu, J., Ming, Q. Z., et al. (2013). Geochemical characteristics and environmental significance of Taledo loess-paleosol sequences of Ili Basin in Central Asia. *Environ. Earth Sci.* 70, 2191–2202. doi: 10.1007/s12665-013-2323-1
- Zhao, Y. L., Feng, X. L., Song, S., and Tian, D. H. (2016). Geochemical partition of surface sediments in the seas near the modern Yellow River Delta. *Mar. Sci.* 40, 98–106. doi: 10.11759/hyxx20160422002
- Zhao, W. C., Liu, L. W., Chen, J., and Ji, J. F. (2019). Geochemical characterization of major elements in desert sediments and implications for the Chinese loess source. *Sci. China-Earth Sci.* 62, 1428–1440. doi: 10.1007/s11430-018-9354-y
- Zhou, L. Y., Liu, J., Saito, Y., Gao, M. S., Diao, S. B., Qiu, J. D., et al. (2016). Modern sediment characteristics and accumulation rates from the delta front to prodelta of the Yellow River (Huanghe). *Geo-Marine Lett.* 36, 247–258. doi: 10.1007/s00367-016-0442-x